Available online at www.sciencedirect.com
SCIENCE DIRECT®
International Journal of Mass Spectrometry 232 (2004) 31–40
International Journal of Mass Spectrometry
www.elsevier.com/locate/ijms

Gas phase nitrosation of substituted benzenes

Noémie Dechamps [a], Pascal Gerbaux [a,1], Robert Flammang [a,*], Guy Bouchoux [b], Pham-Cam Nam [c], Minh-Tho Nguyen [c]

[a] *Organic Chemistry Laboratory, University of Mons-Hainaut, Avenue Maistriau 19, Mons B-7000, Belgium*
[b] *Département de Chimie, Laboratoire des Mécanismes Réactionnels, UMR CNRS 7651, Ecole Polytechnique, Palaiseau Cedex F-91128, France*
[c] *Department of Chemistry, University of Leuven, Celestijnenlaan 200F, Leuven B-3001, Belgium*

Received 22 September 2003; accepted 12 November 2003

Abstract

Using a combination of tandem mass spectrometric experiments (ion–molecule reactions, collisional activation, neutralization–reionization, MS/MS/MS) and theoretical calculations, protonated substituted benzenes are demonstrated to readily react with neutral *t*-butyl nitrite by the formation of stable complexes linking ionized nitric oxide to the benzene derivatives. The overall process is proposed to involve the concomitant elimination of neutral 2-methyl-2-propanol. Proton-bound dimers are proposed to intervene as the key-intermediates in these reactions, which also competitively produce protonated *t*-butyl nitrite. All the experiments were performed in a single hybrid tandem mass spectrometer of sector-quadrupole-sector configuration.

Keywords: Ion–molecule reactions; Collisional activation; Neutralization–reionization; Chemical ionization; Protonated benzenes; Ab initio calculations

1. Introduction

It is now generally accepted that protonated benzene is best described as a C_{2v} σ-protonated structure [1], lying 199 kJ mol^{-1} lower on the $C_6H_7^+$ potential energy surface than the isomeric face-centered π-complex (Scheme 1) [2]. Such species are key-intermediates in electrophilic aromatic substitutions with reaction profiles highly dependent on the nature of electrophiles and reactants.

For instance, nitrosation of benzene is a well-known aromatic electrophilic substitution of a proton by ionized nitric oxide generated by protonation of nitrous acid. The reaction proceeds through π- and σ-adducts with a rate-determining step associated with the deprotonation reaction of the σ-protonated form. This particular behavior has been evidenced by the observation of an isotope effect in the nitrosation of perdeuterated benzene [3]. Recently, theoretical calculations have suggested an alternative to the proposed mechanism involving π-complex transformation into Wheland type σ-structures [4]. The intermediacies of these short-lived σ-protonated forms have been demonstrated by time-resolved spectroscopy [5] and infrared multiphoton decomposition techniques [6].

More recently, we have observed that protonated benzenes readily react with *t*-butyl nitrite (*t*-BuO-N=O), in the quadrupole collision cell of a hybrid tandem mass spectrometer by formal attachment of nitric oxide and simultaneous loss of neutral 2-methyl-2-propanol. The structural determination of the so-produced ions forms the subject of the present report.

2. Experimental

The spectra were recorded on a large-scale tandem mass spectrometer (Micromass AutoSpec 6F, Manchester) combining six sectors of $cE_1B_1cE_2qcE_3B_2cE_4$ geometry (E_i stands for electric sector, B_i for magnetic sector, q for a quadrupole collision cell, and c for conventional collision cells). Typical conditions have been reported elsewhere [7]. The installation of the RF-only quadrupole collision cell (Q cell) inside the instrument between E_2 and E_3 has also been reported [8]. This modification allows the study of associative ion–molecule reactions and the study of low energy (ca. 20–30 eV) collision-induced dissociations of deceler-

* Corresponding author. Tel.: +32-65-373342/44; fax: +32-65-373515.
E-mail address: robert.flammang@umh.ac.be (R. Flammang).
[1] Research associate from the 'Fonds National pour la Recherche Scientifique.'

1387-3806/$ – see front matter © 2003 Elsevier B.V. All rights reserved.
doi:10.1016/j.ijms.2003.11.004

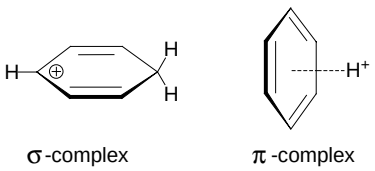

Scheme 1.

ated ions. Briefly, the experiments utilizing the quadrupole consist of the selection of a beam of fast ions (8 keV) with the three first sectors ($E_1B_1E_2$), the deceleration of these ions to approximately 5 eV. The interaction between the ions and the reagent gas is thereafter realized in the Q cell and, after re-acceleration at 8 keV, all the ions generated in the quadrupole are separated and mass measured by scanning the field of the second magnet. The high-energy collisional activation (CA) spectra of mass-selected ions generated in the Q cell can be recorded by a scanning of the field E_4 after selection of the ions with E_3 and B_2.

In the neutralization–reionization experiments, the Q cell and its ion optics is extracted from its housing and an additional neutralization collision cell is inserted before the reionization cell which precedes E_3. Un-reacted ions are eliminated by floating (9000 eV) the intermediate calibration ion source [9].

All the samples were commercially available and used without any further purification.

3. Results and discussion

3.1. Nitrosation of benzene

Proton attachment on benzene readily occurs in the chemical ionization source pressurized with methane. After mass-selection and deceleration at low kinetic energy (see Section 2), these ions react with *t*-butyl nitrite in the RF-only quadrupole collision cell. The product ions, re-accelerated at 8 kV, are thereafter mass analyzed by scanning the field of the second magnetic sector. The resulting spectrum, presented in Fig. 1a, features intense peaks at *m*/*z* 104, 86 and 57 ascribed to proton transfer to *t*-butyl nitrite (MW 103) [10] and, more interestingly, at *m*/*z* 108 for attachment of nitric oxide and loss of a hydrogen atom (probably in the form of 2-methyl-2-propanol), see Scheme 2.

Such $[C_6H_6 + NO]^+$ ions (*m*/*z* 108) have been previously observed in the CI ($NO^\bullet$) mass spectrum of benzene obtained with a Towsend discharge technique [11], or, more recently, in flowing afterglow experiments (selected ion flow tube studies (SIFT)) [12]. The actual structure of these ions was however not defined in these earlier reports but ascribed to π-complexes following other FT-ICR studies [13–15]. Upon collisional activation, the $[C_6H_6 + NO]^+$ ions intensively expel a molecule of nitric oxide and the recorded CA spectrum consequently features a very intense peak at *m*/*z* 78 (Fig. 1b) corresponding to the molecular ions of benzene. The remaining peaks at lower masses are similar to those

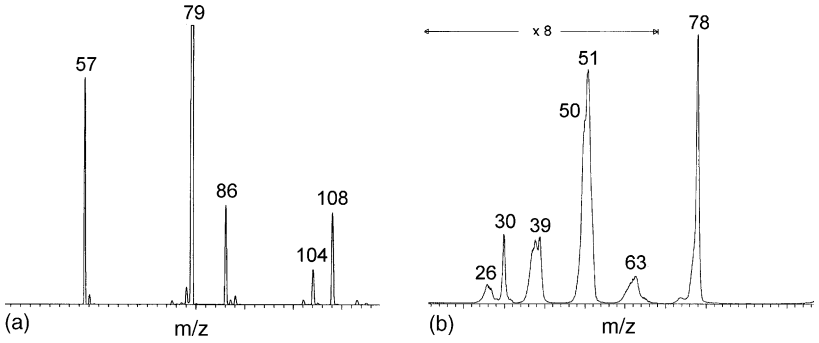

Fig. 1. Ion–molecule reactions of protonated benzene (*m*/*z* 79) with *t*-butyl nitrite (a) and collisional activation spectrum (CA, nitrogen collision gas) of the $[C_6H_6NO]^+$ ions (*m*/*z* 108) (b).

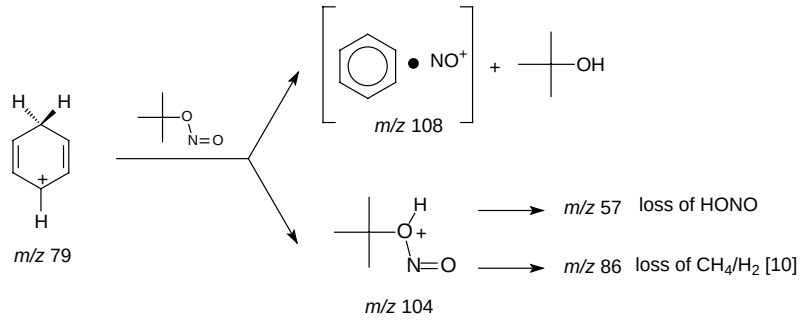

Scheme 2.

observed in the CA spectrum of ionized benzene, except obviously for the *m/z* 30 signal (loss of neutral benzene). All these experimental data support the formation of a cationic adduct connecting nitric oxide to benzene.

Two isotopomers of protonated benzene have been considered in order to evaluate the origin of the leaving hydrogen atom (as 2-methyl-2-propanol). The first species is deuterated benzene ($C_6H_6D^+$, *m/z* 80) obtained by chemical ionization of benzene with CD_3OD as the CI gas, whereas the second cation ($C_6D_6H^+$, *m/z* 85) is prepared by protonation of perdeuterated benzene (CI (methanol)). Both ions are then reacted with *t*-butyl nitrite in the quadrupole cell and we focussed on the NO attachment process. Source conditions were optimized in order to avoid important overlapping of isotopic contaminants. NO^+ attachment is accompanied either by a $H^\bullet$ or a $D^\bullet$ loss. The measured branching ratios are close to the statistical values suggesting that randomization precedes the ion–molecule reactions. Such randomization has also been reported using radiolytic, flowing afterglow and ion cyclotron resonance methodologies [16,17]. Moreover, $H^\bullet$ loss is also seen favored over $D^\bullet$ loss by a significant statistically normalizing factor of 1.6 (ranging from 1.2 to 1.8 in [10]). It has been established by ab initio molecular orbital calculations that the H randomization by 1,2-H shifts connecting two σ-structures of protonated benzene needs only 34 kJ mol^{-1} [1]. Although all gathered evidence points to a σ-structure for protonated benzene, not a face-centered π-complex, the actual structure of the $[C_6H_6 + NO]^+$ ions is not established in these experiments.

The efficiency of neutralization–reionization mass spectrometry in the field of reactive molecules has been demonstrated on numerous occasions (for recent reviews, see [18]). The NR spectrum of the $[C_6H_6 + NO]^+$ ions (*m/z* 108) generated by CI (NO) of benzene is shown in Fig. 2a. No recovery signal corresponding to survivor ions is observed in the recorded spectrum and this experimental fact indicates that the neutral species produced by vertical reduction of the *m/z* 108 ions is characterized by a life time shorter than a fraction of microsecond, that is the time of flight between both the collision cells. The NR spectrum is also very similar to the NR of benzene molecular ions (Fig. 2b), except obviously for the peak at *m/z* 30 (reionized nitric oxide). The following observation is worthy of note when comparing both NR spectra. Although the *m/z* 78 ions formed in the ion source or in the reionization cell have the same kinetic energy (5777 eV), the resolution achieved in the case of the former ions appears significantly increased. It is thus proposed that the reionized species generated during the neutralization–fragmentation–reionization experiment are characterized by a broader distribution of kinetic energies than those produced by direct electron ionization. Diffuse peak shapes have been ascribed to the dissociation products of unstable neutrals [19]. The stability of the cyclohexadienyl radical $[C_6H_7^\bullet]$ prepared by flash photolysis has been recently recognized [20]. Moreover, a series of NR mass spectra of D^+ ring-adducts of aromatic compounds have indicated ion signals for the reionization of the $MD^\bullet$ neutrals [21]. These observations, together with our experimental results, suggest the $[C_6H_6 + NO]^+$ ions to be more likely seen as a face-centered π-complex linking ionized nitric oxide to benzene than as a covalently-bound σ-complex. For the sake of comparison, the NR spectrum of protonated

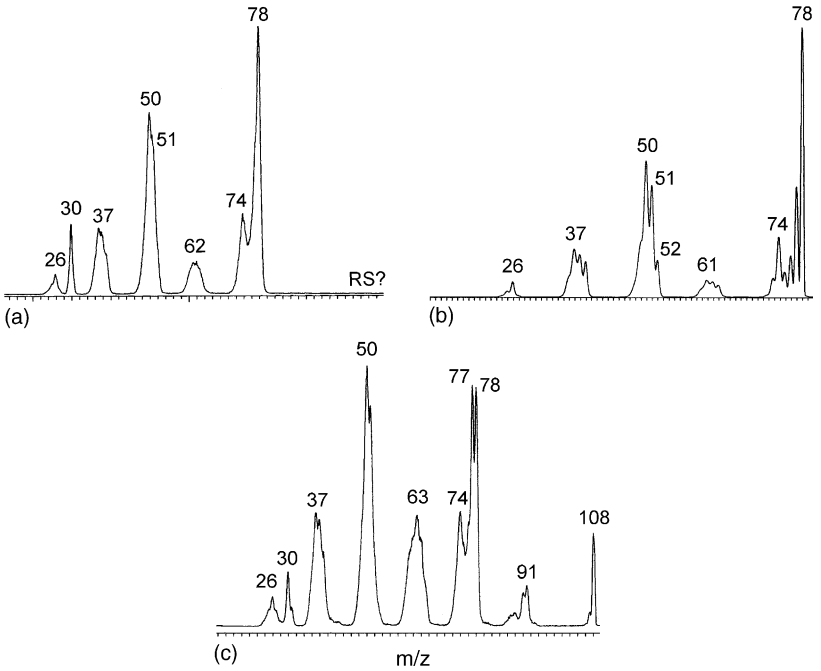

Fig. 2. NR mass spectra (NH_3/O_2) of the $[C_6H_6{}^\bullet NO]^+$ ions (*m/z* 108) (a), of the $[C_6H_6]^{\bullet+}$ radical cations accelerated at 5777 eV (b) and of protonated nitrosobenzene (*m/z* 108) (c).

nitrosobenzene has also been recorded (Fig. 2c); an intense recovery signal is observed at *m*/*z* 108 and the relative abundances of the other peaks are clearly different from those observed in Fig. 2a. Compared to the $[C_6H_6 + NO]^+$ case, vertical reduction of protonated nitrosobenzene generates a stable neutral ascribed to a $C_6H_5N(H)O^\bullet$ nitroxide structure.

In an extensive review, it has been suggested that isomeric σ-structures or π-complexes derived from benzenes could be differentiated on the basis of their reactivity towards appropriate bases [15,22]. σ-Structures are indeed expected to be more prone to react as a Brønstedt acid than π-complexes. We have, therefore, prepared the $[C_6H_6+NO]^+$ in the chemical ionization source (nitric oxide reagent gas) and allowed these ions to react with pyridine in the quadrupole collision cell. In close agreement with a previous result [14], only one significant ionic product was generated in these conditions and originates from the transfer of NO^+ to pyridine (*m*/*z* 109). Consequently, pyridine is characterized by a higher affinity for ionized nitric oxide than benzene. Proton attachment to pyridine (*m*/*z* 80) is not significantly observed (peak intensity of less than 1% of *m*/*z* 109) and this piece of information supports the production of a $[C_6H_6 + NO]^+$ face-centered π-complex ions.

In agreement with the calculations of Skokov and Wheeler [4], at the B3LYP/6-31+G(d,p) level of theory, we were not able to locate a stable σ-structure for the $[C_6H_6 + NO]^+$ species. Irrespective of the initially selected structure, the super-system always converged toward the π-complex with a stretching of the C–N bond and a displacement of NO^+ toward the π-position. The final structure, depicted in Fig. 3a, is stabilized by 195 kJ mol^{-1} relative to the isolated nitrosonium cation plus neutral benzene. The bond distances in the

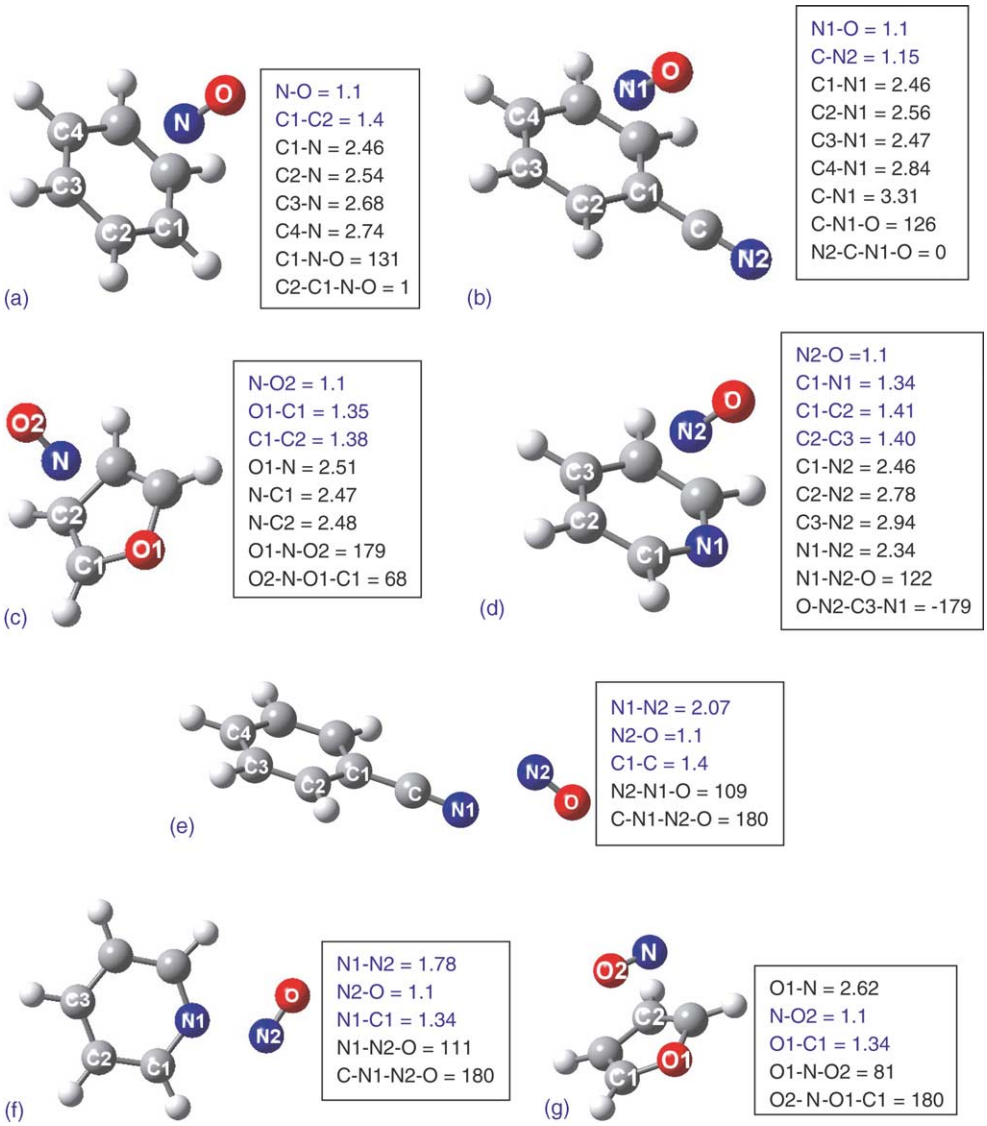

Fig. 3. Optimized geometry (B3LYP/6-31+G(d,p)) of the face-centered π-complexes connecting ionized nitric oxide to (a) benzene, (b) phenyl cyanide, (c) pyridine and (d) furan and optimized geometry at the same level of theory of the *n*-complexes connecting ionized nitric oxide to (e) pyridine, (f) phenyl cyanide, and (g) furan. Bond lengths are given in angstroms (Å) and bond angles in degrees (°).

Table 1
Relative abundance (%) of ions generated during the interaction of protonated aromatic species and *t*-butyl nitrite in the quadrupolar collision cell

Substances	PA[a] (kJ mol^{-1})	NO$^{\bullet}$ attachment	"*t*-Butyl" attachment	Protonation of the nitrite	ΔH[b] (kJ mol^{-1})
Nitrobenzene	809	44	2	54	−55
Phenyl cyanide	820	48	8	44[c]	−44
Benzaldehyde	838	61	–	39	−26
Me benzoate	852	86	–	14	−12
Acetophenone	859	98	–	2	−5

[a] Proton affinities (kJ mol^{-1}) [25].
[b] Heats of reaction based on the 864 kJ mol^{-1} proton affinity of *t*-butyl nitrite [26].
[c] Hidden reaction: roughly estimated assuming that *m*/*z* 104 and 86 have similar intensities.

benzene ring are only scarcely modified by the presence of the NO^+ cation. It is also worthy of note that the N–O bond is not rigorously perpendicular to the ring. This spatial arrangement actually avoids an unstable symmetrical pyramidal arrangement [23] which could cause a degeneracy of the electronic configuration. A Jahn–Teller-type distortion leads to a stabilized structure having a lower symmetry.

3.2. Nitrosation of substituted benzenes

Similar experiments have been extended to the case of various mono-substituted benzenes: nitrobenzene, phenyl cyanide, benzaldehyde, acetophenone and methyl benzoate. A common feature of these compounds is that they suffer protonation on the substituent, not on the ring, under chemical ionization conditions [24]. Phenyl cyanide will be used in the present report as a prototype and all the results concerning this particular compound have been nicely reproduced for the other phenyl derivatives.

3.2.1. Preparation by ion–molecule reactions

The results of the ion–molecule reactions between *t*-butyl nitrite and the protonated aromatics are summarized in Table 1 and illustrated in Fig. 4 in the specific case of phenyl cyanide. Attachment of NO$^{\bullet}$ followed by the loss of a hydrogen atom is an important process formally corresponding to 2-methyl-2-butanol elimination. The second reaction of importance is the proton transfer to *t*-butyl nitrite, but its relative importance is rapidly decreasing when the proton affinity of the substituted benzenes increases. *t*-Butyl attachment (formal loss of nitrous acid from the encounter complex) is also observed as a minor reaction for protonated nitrobenzene and protonated phenyl cyanide. Peaks for NO$^{\bullet}$ attachment are not shifted in labeling

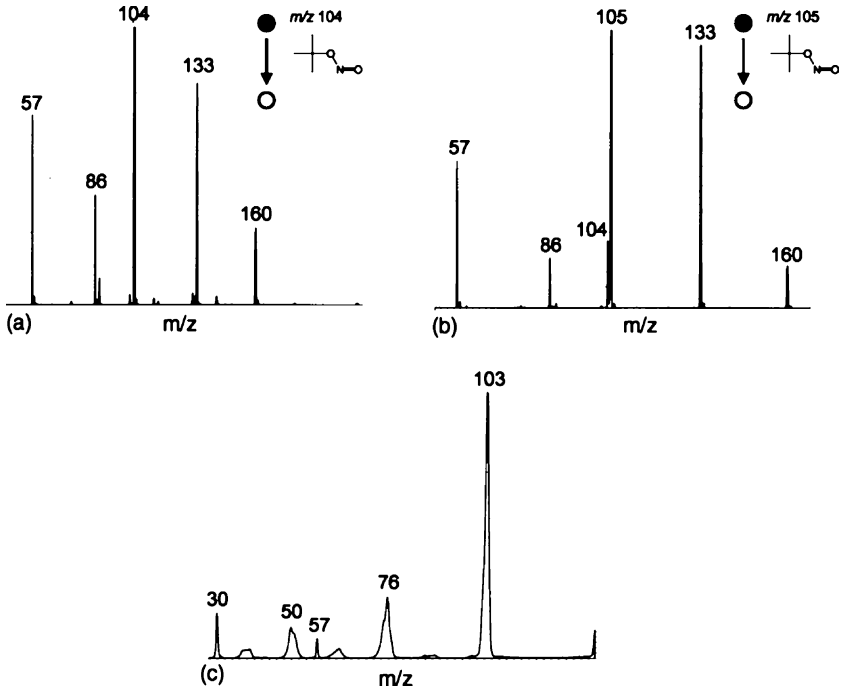

Fig. 4. Ion–molecule reactions of ions derived from phenyl cyanide with *t*-butyl nitrite. (a) Protonated phenyl cyanide (*m*/*z* 104)/*t*-butyl nitrite; (b) deuterated phenyl cyanide (*m*/*z* 105)/*t*-butyl nitrite. Peaks corresponding to incident ions are off-scale; (c) CA spectrum (nitrogen collision gas) of the *m*/*z* 133 ions observed in (a).

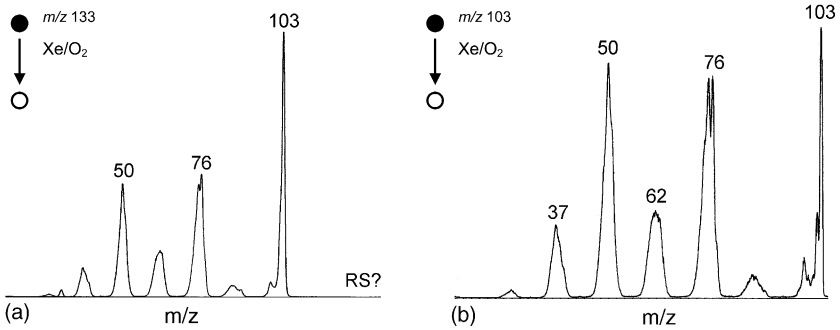

Fig. 5. NR spectra (xenon/oxygen) of the *m*/*z* 133 ions generated by chemical ionization ($NO^{\bullet}$) of phenyl cyanide (a) and of the molecular ions (*m*/*z* 103) of phenyl cyanide accelerated at 6195 eV (b).

experiments using perdeuterated methanol as the CI reagent gas indicating that, in contrast with the benzene case, the deuterium atom is specifically expelled in the process (as *O*-deuterated 2-methyl-2-butanol).

Collisional activation in the high (8 keV) kinetic regime indicates that the major process is the dissociation of the complexes into the corresponding ionized substituted benzene and $NO^{\bullet}$. The resulting spectra thus resemble the CA spectra of the corresponding benzenes plus a less intense peak at *m*/*z* 30 for NO^+ ions. As seen in Fig. 4c for the phenyl cyanide case, the peak at *m*/*z* 57 is due to the dissociation of a small quantity of isobaric ions coming from nitrosation of *t*-butyl nitrite itself.

3.2.2. Neutralization–reionization experiments

The NR spectrum of the $[C_6H_5CN+NO]^+$ ions (*m*/*z* 133) generated by CI ($NO^{\bullet}$) of phenyl cyanide is shown in Fig. 5a. As for the benzene case (vide supra), no recovery signal is observed indicating that the neutral radical $[C_6H_5CN+NO]^{\bullet}$ was generated transiently in the gas phase by vertical reduction of the mass-selected ions and immediately—within a fraction of microsecond—dissociates into phenyl cyanide and nitric oxide. Subsequent collision-induced reionization of both these neutral molecules yields the NR spectrum shown in Fig. 5a that consequently is found very similar to the NR spectrum of phenyl cyanide radical cations (Fig. 5b) except for the signal at *m*/*z* 30 corresponding to reionized nitric oxide.

Similar results were obtained for $[C_6H_5NO_2 + NO]^+$ ions (*m*/*z* 153) and $[C_6H_5COCH_3 + NO]^+$ ions (*m*/*z* 150). $[C_6H_5CHO + NO]^+$ ions (*m*/*z* 136) and $[C_6H_5CO_2CH_3 + NO]^+$ ions (*m*/*z* 166) behave in NRMS experiments as do the other ions: complete absence of recovery signals and NR spectra very similar to the CA spectra of the derived radical cations.

3.2.3. Quantum chemical calculations

As in the case of benzene itself, we have identified at the B3LYP/6-31+G(d,p) level of theory a stable π-complex, depicted in Fig. 3b, stabilized by 131 kJ mol^{-1} relative to the isolated nitrosonium cation plus neutral phenyl cyanide. The bond distances in the benzene ring are only scarcely modified by the presence of the NO^+ cation. It is also worthy of note that the N–O bond is not again rigorously perpendicular to the ring; this is probably caused by the non-symmetric charge distribution in NO^+. Further experiments (see below) will nevertheless indicate that *this π-complex is not the most stable* complex.

3.2.4. Ion–molecule reactions with pyridine, benzene and furan

As already mentioned, chemical ionization of substituted benzenes using *t*-butyl nitrite as the reagent gas has allowed in all cases the production of $[M + NO]^+$ ions within the ion source. These ions react efficiently with pyridine in the quadrupole collision cell by transfer of NO^+ to pyridine (production of *m*/*z* 109 ions, see Table 2). A very small amount of protonated pyridine (*m*/*z* 80) is only observed in the case of benzaldehyde. As for benzene itself, this seems to indicate that the $[M+NO]^+$ ions formed are not σ-complexes that are expected to act as Brønsted acid by proton transfer reactions. The reacting $[M + NO]^+$ have also been prepared by nitric oxide chemical ionization, except for benzaldehyde which reacts exclusively by hydride abstraction and methyl benzoate which reacts mainly by methoxide abstraction. In these ionization conditions, the transfer of NO^+ to pyridine was also found the dominant process.

Since pyridine is a π-deficient system, it also appeared of interest to investigate two others reagents, namely neutral furan (a π-exceedingly heterocyclic system) and neutral benzene. As in the case of pyridine, all the different complexes transferred NO^+ to the neutral reagents (see Table 2). The NO transfer was the most efficient process when pyridine is the target compound except in the cases of nitrobenzene and phenyl cyanide complexes where the efficiencies were found to be quite similar irrespective of the nature of the reactive ion.

The $[pyridine + NO]^+$, $[furan + NO]^+$ and $[benzene + NO]^+$ complexes could also readily be formed under nitric oxide chemical ionization conditions. The structure of the π-complexes calculated at the B3LYP/6-31+G(d,p) level of theory has already been described in Fig. 3. Their relative stabilities have been estimated by crossed reactions with their corresponding neutrals (see Table 3). It is exper-

Table 2
Ion–molecule reactions of $[M + NO]^+$ ions with pyridine, furan or benzene in the quadrupolar collision cell

Reacting $[M + NO]^+$ ions	Neutral reagents	Efficiency[a] (%)	Other ions *m/z* (%)[b]
M = nitrobenzene	Pyridine	8	30 (1)
	Furan	9	68 (5)
	Benzene	6	30 (10), 78 (2)
Phenyl cyanide	Pyridine	14	79 (0.1), 30 (0.1)
	Furan	22	68 (9), 30 (0.4)
	Benzene	11.5	78 (1), 30 (0.4)
Benzaldehyde	Pyridine	21	105 (26), 80 (3), 79 (2)
	Furan	2	105 (120), 68 (3)
	Benzene	1	105 (276), 30 (<1)
Me benzoate	Pyridine	22	105 (13)
	Furan	3	105 (97), 68 (0.7)
	Benzene	3	105 (106)
Acetophenone	Pyridine	12	120 (2)
	Furan	0.5	120 (48), 68 (6), 108 (8)
	Benzene	0.3	120 (112), 30 (22), 78 (5)

[a] Abundance of *m/z* 109 $[pyridine + NO]^+$, 98 $[furan + NO]^+$ or 108 $[benzene + NO]^+$ ions relative to un-reacted ions.
[b] Abundance relative to *m/z* 109 $[pyridine + NO]^+$, 98 $[furan + NO]^+$ or 108 $[benzene + NO]^+$ ions.

imentally found that the NO^+ affinity decreases in the order pyridine > furan > benzene. However, the fact that the $[pyridine + NO]^+$ complex does not transfer significantly ionized NO to furan and benzene is in apparent contradiction with the calculated negative heats of reactions reported in the fourth column of Table 4. It was therefore suspected that the π-$[pyridine + NO]^+$ complex was not the most stable structure and the occurrence of *n*-complexation, namely an interaction with the nitrogen lone pair of electrons, has therefore to be taken into account.

Calculations at the B3LYP/6-311++G(d,p) level of theory reveal that both the π- and *n*-$[pyridine + NO]^+$ adducts are true local minima on the potential energy surface. The *n*-complex turns out to be more stable by about 96 kJ mol^{-1} than the π-complex explaining thus the results indicated in the fifth column of Table 4. Similar calculations on π- and *n*-$[phenyl\ cyanide + NO]^+$ complexes also revealed a better stabilization of the *n*-complex (31 kJ mol^{-1} compared to the π-complex). In the case of furan, NO appears to lie in a plane parallel to the heterocycle (see Fig. 3g). We note that the N1–N2 distance in the *n*-$[C_6H_5CN + NO]^+$ adduct of 2.07 Å (Fig. 3e) is longer than that of 1.78 Å in the *n*-$[pyridine + NO]^+$ adduct counterpart (Fig. 3f). In both cases, these longer distances indicate the complex character of the adducts.

In order to confirm the higher stability of the *n*-complex, we have carried out coupled-cluster theory calculations, on both π- and *n*-complexes of the $[phenyl\ cyanide + NO]^+$ system. At the CCSD(T)/6-311++G(d,p) level of theory, the *n*-complex (Fig. 3e) is in fact found to be 28 kJ mol^{-1} below the π-complex (Fig. 3b). This result lends further support for the B3LYP-values obtained for other complex systems.

Table 3
Ion–molecule reactions of $[pyridine+NO]^+$, $[furan+NO]^+$ and $[benzene+NO]^+$ ions with neutral pyridine, furan or benzene in the quadrupolar collision cell

Reacting $[M + NO]^+$ ions	Neutral reagents	Efficiency[a] (%)
M = phenyl cyanide	Furan	22
Benzene		3.5
Pyridine		<0.1
Phenyl cyanide	Benzene	11.5
Furan[b]		3
Pyridine		0.1
Phenyl cyanide	Pyridine	14
Benzene		3.5
Furan[b]		3

[a] Abundance of *m/z* 109 $[pyridine + NO]^+$, 98 $[furan + NO]^+$ or 108 $[benzene + NO]^+$ ions relative to un-reacted ions.
[b] Complexes prepared by CI of a mixture of furan and *t*-butylnitrite.

3.2.5. Mechanisms

As proposed in Scheme 3, proton-bound dimers are most probably involved in the observed ion–molecule reactions. Nevertheless, such intermediate species is never observed in the quadrupole collision cell probably due to the lack of thermalization. In the case of nitrobenzene and phenyl cyanide, these dimers can however be produced in the chemical ionization source—ionization of a mixture of the aromatic species and *t*-butyl nitrite—and their collisional activation supports their intervention in the processes. This is indicated by the CA spectrum of the *m/z* 221 ions generated during methanol chemical ionization of a mixture of *o*-methyl phenyl cyanide (this cyanide was choosen in order to eliminate isobaric ambiguities) and *t*-butyl nitrite which, as expected [28], mainly dissociate yielding competitively the protonated forms of both partners—protonated *t*-butyl nitrite and protonated *o*-methyl phenyl cyanide are respectively observed at *m/z* 104 and 118. It is also observed in this CA spectrum an intense signal at *m/z* 147 corresponding

Table 4
Transfer reactions of NO^+ from π-complexes to neutral furan (theoretical and experimental results)

Complexes	Neutral reagent	NO^+ transfer to neutral reagent[a]	ΔH (kJ mol^{-1})[b] π-complex	ΔH (kJ mol^{-1})[c] *n*-complex
Pyridine	Furan	Not observed	−35	59
Phenyl cyanide		Observed	−42	−14
Benzene		Observed	4	3
Pyridine	Benzene	Not observed	−38	56
Phenyl cyanide		Observed	−47	−17
Phenyl cyanide	Pyridine	Observed	−9	−73

[a] Experimental results.
[b] Heats of reaction based on the calculations of the different π-complexes at the B3LYP/6-31+G(d,p), B3LYP/6-311+G(2df,p) and MP2/6-311+G(2df,p) level of theory.
[c] Heats of reaction based on the calculations of the different *n*- and π-complexes at the B3LYP/6-311++G(d,p) level of theory.

to the transfer of NO^+ cation to methylphenyl cyanide, see Scheme 3 (relative abundances of the *m*/*z* 104, 118 and 147: 24, 56 and 20% respectively). All these experimental data reveal that *m*/*z* 221 cations are likely to be the key-species on the way to the formation of the observed ion–molecule reaction products.

We have then established, by quantum chemical calculations at the B3LYP/6-311++G(d,p) level of theory, a potential energy diagram (see Fig. 6) related to the reactions of protonated phenyl cyanide with *t*-butyl nitrite—protonation of the nitrite (*m*/*z* 104), *n*-adduct (*m*/*z* 133) and *t*-butylation of phenyl cyanide (*m*/*z* 160). The heats of reactions depicted in the diagram are in agreement with the observation of the ion–molecule reactions experimentally observed (see Table 2). Proton transfer to the *t*-butyl nitrite appears to be slightly endothermic, while the two other processes are calculated to be very slightly exothermic. Under our experimental conditions (absence of efficient thermalization of the reactive mass-selected ions prior to the interaction), low energy barriers are certainly easily surmounted. At the B3LYP/6-311++G(d,p) level of theory, we were not able to localize the proton-bound complex; the value (−82 kJ mol^{-1}) given in Fig. 6 corresponds to a calculated stabilization energy of the phenyl cyanide/methyl nitrite proton-bound complex.

Finally, it is worth noting that the structure of the *m*/*z* 160 ion, initially considered as *N*-*t*-butyl phenyl cyanide, is more likely a "proton-bound dimer species" in which a proton is *solvated* by a molecule of phenyl cyanide and a molecule of 2-methylpropene. At the B3LYP/6-311++G(d,p) level of theory, we were not able to localize a stable *N*-*t*-butyl phenyl cyanide structure.

The *n*-complex represents thus a global minimum on the potential energy surface of the cation NO^+/phenyl cyanide system (see Fig. 6). The stabilization of the nitrosonium cation by complexation by a molecule of phenyl cyanide amounts to 178 kJ mol^{-1}. Together with the heats of formation of phenyl cyanide (219 kJ mol^{-1}) and NO^+

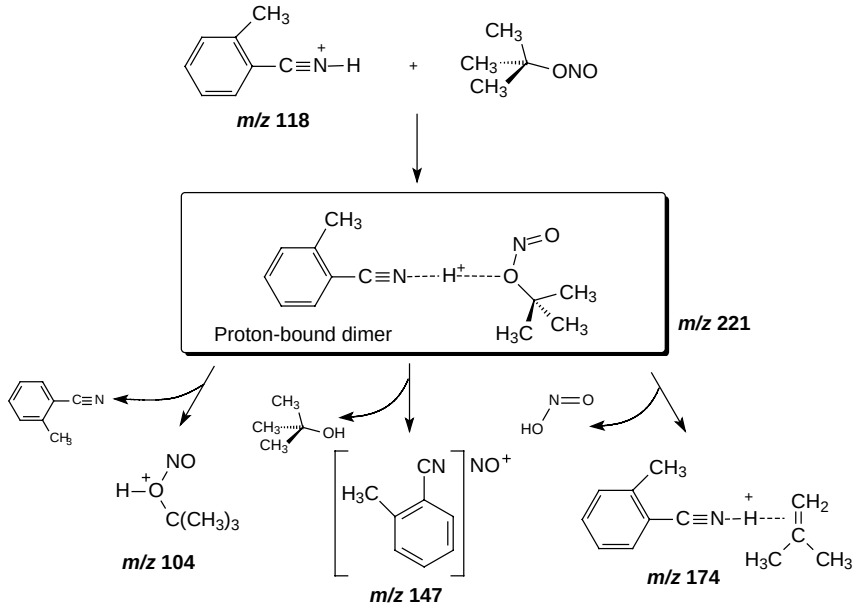

Scheme 3.

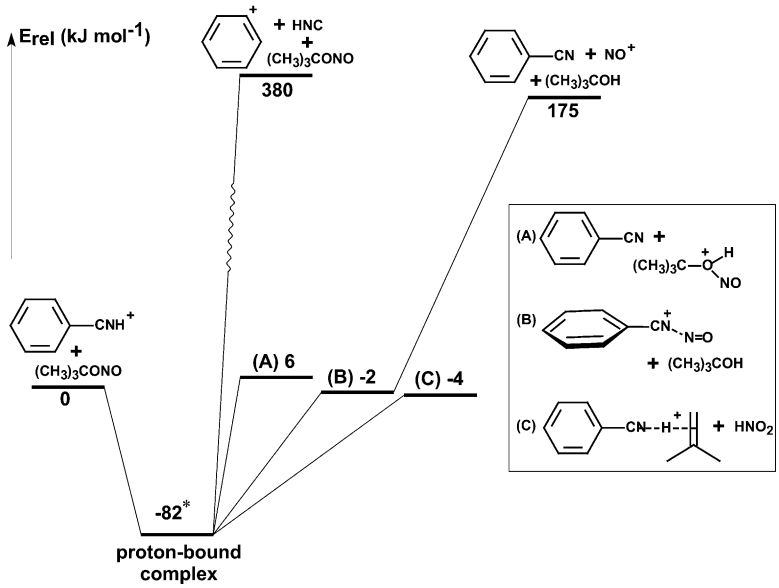

Fig. 6. Potential energy diagram for the reaction of protonated phenyl cyanide with *t*-butyl nitrite (energies in kJ mol^{-1}).

(984 kJ mol^{-1}) [25], the heat of formation of the *n*-complex is estimated to be 1025 kJ mol^{-1}. A comparison of all these theoretical data and experimental literature data suggest that reported [27] heats of formation and proton affinities of nitrites need to be re-evaluated.

4. Conclusions

Using a combination of experimental tandem mass spectrometric methods (ion–molecule reactions, collisional activation, neutralization–reionization) and quantum chemical calculations, it is shown that protonated benzene reacts efficiently with *t*-butyl nitrite with the production of $[C_6H_6 + NO]^+$ ions consisting of a face-centered π-complex connecting nitric oxide to benzene. Substituted benzenes, being protonated on the substituent, not on the ring, behave similarly but the binding of ionized nitric oxide (*n*-complexes) appears more stabilizing than π-complexation. Neutral 2-methyl-2-propanol eliminated in this process effectively "transports" NO^+ from the nitrite to the benzenes in this reaction. An experimental reevaluation of the available thermochemical data of nitrites seems to be greatly required.

Acknowledgements

The Mons laboratory thanks the "Fonds National de la Recherche Scientifique" (FNRS) for financial support in the acquisition of the hybrid tandem mass spectrometer. M.T.N. is indebted to the FWO-Vlaanderen and the Flemish Government (GOA program) for continuing support.

References

[1] (a) M.N. Glukhovtsev, A. Pross, A. Nicolaides, L. Radom, J. Chem. Soc. Chem. Commun. 22 (1995) 2347;
(b) Z.B. Maksic, B. Kovacevic, A. Lesar, Chem. Phys. 253 (2000) 59.
[2] R.S. Mason, C.M. Williams, P.D.J. Anderson, J. Chem. Soc. Chem.Commun. 10 (1995) 1027.
[3] B.C. Challis, R.J. Higgins, A.J. Lawson, J. Chem. Soc. Perkin Trans. 2 (1972) 1831.
[4] S. Skokov, R.A. Wheeler, J. Phys. Chem. A 103 (1999) 4261.
[5] S.M. Hubig, J.K. Kochi, J. Am. Chem. Soc. 122 (2000) 8297.
[6] W. Jones, P. Boissel, B. Chiavarino, M.E. Grestoni, S. Fornarini, J. Lemaire, P. Maitre, Angew. Chem. 115 (2003) 2103.
[7] R.H. Bateman, J. Brown, M. Lefevere, R. Flammang, Y. Van Haverbeke, Int. J. Mass Spectrom. Ion Process. 115 (1992) 205.
[8] R. Flammang, Y. Van Haverbeke, C. Braybrook, J. Brown, Rapid Commun. Mass Spectrom. 9 (1995) 795.
[9] J. Brown, R. Flammang, Y. Govaert, M. Plisnier, C. Wentrup, Y. Van Haverbeke, Rapid Commun. Mass Spectrom. 6 (1992) 249.
[10] R. Farid, T.B. Mc Mahon, Int. J. Mass Spectrom. Ion Phys. 27 (1978) 163.
[11] S. Daishima, Y. Iida, F. Kanda, Org. Mass Spectrom. 26 (1991) 486.
[12] (a) P. Spanel, D. Smith, Int. J. Mass Spectrom. 181 (1998) 1;
(b) D. Smith, T. Wang, P. Spanel, Int. J. Mass Spectrom. 230 (2003) 1.
[13] W.D. Reents, B.S. Freiser, J. Am. Chem. Soc. 102 (1980) 271.
[14] W.D. Reents, B.S. Freiser, J. Am. Chem. Soc. 103 (1981) 2791.
[15] F. Cacace, A. Ricci, Chem. Phys. Lett. 253 (1996) 184.
[16] B. Chiavarino, M.E. Crestoni, C.H. DePuy, S. Fornarini, R. Gareyev, J. Phys. Chem. 100 (1996) 16201.
[17] C.H. DePuy, R. Gareyev, S. Fornarini, Int. J. Mass Spectrom. Ion Process. 161 (1997) 41.
[18] (a) C.A. Schalley, G. Hornung, D. Schröder, H. Schwarz, Chem. Soc. Rev. 27 (1998) 91;
(b) F. Turecek, Top. Curr. Chem. 225 (2003) 77.
[19] D.V. Zagorevskii, J.L. Holmes, Eur. Mass Spectrom. 3 (1997) 317.

[20] F. Berho, M.T. Rayez, R. Lesclaux, J. Phys. Chem. A 103 (1999) 5501.
[21] A.W. McMahon, F. Chadikun, A.G. Harrison, R.E. March, Int. J. Mass Spectrom. Ion Process. 87 (1989) 275.
[22] M. Speranza, Int. J. Mass Spectrom. Ion Process. 118 (1992) 395.
[23] G.I. Borodkin, V.G. Shubin, Russ. Chem. Rev. 70 (2001) 211.
[24] Y. Lau, P. Kebarle, J. Am. Chem. Soc. 98 (1976) 7452.
[25] S.G. Lias, J.E. Bartmess, J.F. Liebman, J.L. Holmes, R.D. Levin, W.G. Mallard, J. Phys. Chem., 17 (Suppl. 1) (1988) (reference data).
[26] E.P. Hunter, S.G. Lias, J. Phys. Chem. 27 (1998) 413 (reference data).
[27] http://webbook.nist.gov/
[28] R.G. Cooks, J.S. Patrick, T. Kotiaho, S.A. McLuckey, Mass Spectrom. Rev. 13 (1994) 287.